



# UNIVERSITÀ DI PARMA

## ARCHIVIO DELLA RICERCA

University of Parma Research Repository

Computational fluid dynamics (CFD) modelling and experimental validation of thermal processing of canned fruit salad in glass jar

This is the peer reviewed version of the following article:

*Original*

Computational fluid dynamics (CFD) modelling and experimental validation of thermal processing of canned fruit salad in glass jar / Cordioli, Matteo; Rinaldi, Massimiliano; Copelli, Gabriele; Casoli, Paolo; Barbanti, Davide. - In: JOURNAL OF FOOD ENGINEERING. - ISSN 0260-8774. - 150:(2015), pp. 62-69. [10.1016/j.jfoodeng.2014.11.003]

*Availability:*

This version is available at: 11381/2783476 since: 2018-04-16T10:31:12Z

*Publisher:*

Elsevier Ltd

*Published*

DOI:10.1016/j.jfoodeng.2014.11.003

*Terms of use:*

Anyone can freely access the full text of works made available as "Open Access". Works made available

*Publisher copyright*

note finali coverpage

(Article begins on next page)

Manuscript Number: JFOODENG-D-14-00230

Title: Computational Fluid Dynamics (CFD) Modelling and Experimental Validation of Thermal Processing of Canned Fruit Salad in Glass Jar

Article Type: Research Article

Keywords: CFD; Thermal processing; Canned fruit salad; Natural convection; Conduction.

Corresponding Author: Prof. Davide Barbanti,

Corresponding Author's Institution: University of Parma - Italy -

First Author: Matteo Cordioli

Order of Authors: Matteo Cordioli; Massimiliano Rinaldi; Gabriele Copelli; Paolo Casoli; Davide Barbanti

Abstract: In this study, samples of commercial fruit salad (five different fruits with various geometries and thermal properties) were used for the experiments in order (i) to study the thermal behaviour of fruits during the heat treatment and (ii) to develop a computational fluid dynamics model to investigate the temperature profiles during samples processing. Simulation data were validated with the experimental ones obtained by means of a pilot plant. Results showed a good fit between theoretical and experimental data, both for syrup and fruit pieces. Experimental F values varied as a function of the type of fruit, its position, dimension and thermal property and they were shown to be influenced by the natural convection motion of the syrup. The proposed model can be used for the simulation and prediction of thermal processes of canned fruit salad, though better reliability (by reducing the differences between theoretical and experimental data and by studying the influence of fruit position inside the jar during the thermal process) can be achieved.



UNIVERSITA' DEGLI STUDI DI PARMA

DIPARTIMENTO DI SCIENZE DEGLI ALIMENTI

Department of Food Science

[www.unipr.it](http://www.unipr.it)

Parco Area delle Scienze, 47/A  
43124 Parma - Italia  
Tel. +39 0521 90 5706

To: Editor-in-Chief of Journal of Food Engineering

Dear Professor,

I would like to submit to your attention a research paper on "Computational Fluid Dynamics (CFD) Modelling and Experimental Validation of Thermal Processing of Canned Fruit Salad in Glass Jar", by *M.Cordioli, M.Rinaldi, G.Copelli, P.Casoli and D.Barbanti*, for the publication in the Journal of Food Engineering.

As reported in the instruction for authors, the manuscript has been deeply reviewed by a native English speaker.

Each decision and suggestion from you and referees will be useful to us in order to improve the scientific quality of the paper.

Parma, 02.25.2014

With my Best Regards

Davide Barbanti

A handwritten signature in blue ink that reads "Barbanti Davide".

## Highlights

Heat distribution was optimized during thermal treatment of fruit salad

A computational fluid dynamics model was used to investigate the temperature profiles

Simulation data were validated with those of experimental trials

The CFD model can be used for the simulation and prediction of thermal processes

1        **Computational Fluid Dynamics (CFD) Modelling and Experimental Validation of Thermal**  
2                                **Processing of Canned Fruit Salad in Glass Jar**

3

4        Matteo Cordioli<sup>1</sup>, Massimiliano Rinaldi<sup>1</sup>, Gabriele Copelli<sup>2</sup>, Paolo Casoli<sup>2</sup>, Davide Barbanti<sup>1\*</sup>

5

6        <sup>1</sup>Department of Food Science, University of Parma, Parco Area delle Scienze 47/A, 43124 Parma,

7        Italy

8        <sup>2</sup>Department of Industrial Engineering, University of Parma, Parco Area delle Scienze 181/A,

9        43124 Parma, Italy

10

11

12

13        \*Corresponding author: Davide Barbanti, Department of Food Science, Parco Area delle Scienze

14        47/A, 43124 Parma, Italy. Tel: 0039-521-905706; e-mail: [davide.barbanti@unipr.it](mailto:davide.barbanti@unipr.it)

15 **Abstract**

16 In this study, samples of commercial fruit salad (five different fruits with various geometries and  
17 thermal properties) were used for the experiments in order (i) to study the thermal behaviour of  
18 fruits during the heat treatment and (ii) to develop a computational fluid dynamics model to  
19 investigate the temperature profiles during samples processing. Simulation data were validated with  
20 the experimental ones obtained by means of a pilot plant. Results showed a good fit between  
21 theoretical and experimental data, both for syrup and fruit pieces. Experimental *F values* varied as a  
22 function of the type of fruit, its position, dimension and thermal property and they were shown to be  
23 influenced by the natural convection motion of the syrup. The proposed model can be used for the  
24 simulation and prediction of thermal processes of canned fruit salad, though better reliability (by  
25 reducing the differences between theoretical and experimental data and by studying the influence of  
26 fruit position inside the jar during the thermal process) can be achieved.

27

28

29

30 **Keywords:** CFD, Thermal processing, Canned fruit salad, Natural convection, Conduction.

31 **1.Introduction**

32 In the food industry, a great number of fruits and vegetables are packaged in cans or jars, filled with  
33 an appropriate sugar syrup or brine, and thermally processed in order to increase their shelf life  
34 through the inactivation of both spoilage microorganisms and enzymes (Kiziltas et al., 2010).

35 Heat transfer mechanisms in canned food are conduction for solid and high viscosity liquid foods,  
36 natural convection for low viscosity liquid foods, convection plus conduction for liquid foods with  
37 solid particles and convection followed by conduction for liquid foods containing starch or viscosity  
38 modifiers (Chen and Ramaswamy, 2007).

39 Moreover, it is widely known that quality as well as nutritional characteristics of foods can be  
40 dramatically reduced by the thermal stabilisation processes. Hence, time and temperature  
41 combination during the heating and the cooling cycles must be properly assessed to guarantee both  
42 effectiveness (inactivation of microorganisms and enzymes) and efficiency (retention of sensory  
43 and nutritional characteristics as well as limiting of costs). As a consequence, the thermal process  
44 must be properly designed by studying the thermal properties of foods and the mechanism of heat  
45 transfer during the treatment. These purposes are normally achieved by a relevant number of  
46 experimental trials with an increase in costs and time consumption thus reducing the possibility to  
47 have fast, efficient and in-depth results (Sun, 2007).

48 In order to overcome these limits, in the last years, process design in the food industry has been  
49 increasingly carried out by using numerical solutions of process governing equations, modelling  
50 and calculation methods (Weng, 2005).

51 Among these, Computational Fluid Dynamics (CFD), has found widespread application in many  
52 areas of food processing such as spray drying, baking, sterilization, heat exchangers design,  
53 chilling, mixing, fermentation and in the agri-food industry (Sun, 2007).

54 CFD is a simulation tool which uses powerful computers and applied mathematics to model fluid  
55 flow situations for the prediction of heat, mass, momentum transfer and optimal design in industrial

56 processes (Xia and Sun, 2002; Kuriakose and Anandharamakrishnan, 2010; Anandharamakrishnan,  
57 2011; Chhanwal et al., 2012). Several works deal with CFD simulations of canned foods: Kumar et  
58 al. (1990) simulated the natural convection in canned thick viscous liquid foods; Ghani et al.  
59 (1999a, 2002) studied the natural convection heating of canned foods in vertical and horizontal  
60 positions, showing faster heating in the vertical can, which is expected due to the enhancement of  
61 natural convection caused by its greater height. The effect of the inclination of container walls and  
62 geometry modification on the sterilization process was also investigated by Varma and Kannan  
63 (2005).

64 A few works have been published on the CFD simulation studies of canned foods with solid/liquid  
65 mixture. These include heat transfer and liquid flow prediction during the sterilization of large  
66 particles in a cylindrical vertical can (Rabiey et al., 2007) and the heat transfer in canned peas under  
67 pasteurization (Kiziltas et al., 2010). Ghani and Farid (2006) analysed and successfully modelled  
68 the thermal sterilization process of canned solid-liquid food mixture (pineapple slices with  
69 governing liquid) in metal cans, indicating that natural convection effects in the liquid played a  
70 significant role in the evolution of temperature. In the same way, Dimous and Yanniotis (2011)  
71 studied the temperature profile, the velocity profile and the slowest heating zone in a still can filled  
72 with food items with cylindrical-conical shape such as asparagus. With regard to pineapples,  
73 Padmavati and Anandharamakrishnan (2013) investigated the effect of size reduction of the product  
74 (pineapple slices vs. tidbits) on the effectiveness of heat transfer during thermal processing.

75 However, the scientific literature still lacks a comprehensive simulation study for the prediction of  
76 temperature changes of solid-liquid mixtures where solids with different shapes and thermal  
77 characteristics are dispersed in the liquid phase.

78 In this paper, samples of commercial fruit salad (composed of five different fruits with various  
79 geometries and thermal properties) were canned in glass jars and submitted to heat treatment.



80 The objectives of this work were (i) to study the temperature distribution and the thermal behaviour  
81 of both fruit pieces and syrup during the process and (ii) to develop and experimentally validate a  
82 computational fluid dynamics (CFD) model of the process itself.

83

## 84 **2. Materials and Methods**

### 85 *2.1 Plant and process details*

86 The thermal treatment of fruit salad and sugar syrup in a glass jar was carried out in a small scale  
87 static pasteuriser (JBT FoodTech, Parma, Italy), controlled by PLC. Inside the pasteuriser (width =  
88 550 mm; length = 730 mm) water was sprayed over the containers from two nozzles at a rate of  
89  $2800 \text{ l}\cdot\text{h}^{-1}$  with a spread angle of  $120^\circ$ . Hot water temperature was set at  $93^\circ\text{C}$  and samples were  
90 heated from  $22$  to  $85^\circ\text{C}$  at the slowest heating point (SHP). The water was heated and cooled  
91 through a “tube in tube” heat exchanger where the heating and cooling media were water vapour  
92 and icy water, respectively. The jar was positioned at the centre of the pasteuriser between the  
93 nozzles and was surrounded with other jars (filled with the same product) in order to reproduce the  
94 operating conditions of the industrial process.

95 During trials, only the heating phase of the thermal processing was studied.

96

### 97 *2.2 Sample characteristics*

98 The fruit salad was composed of five different fruits (percentage expressed by weight): peach  
99 (52%), pear (38%), pineapple (5%), grape (3%) and cherry (2%). Peach and pear were cubic with  
100 sides of 10 and 8 mm, respectively. Pineapple had a truncated pyramid geometry (such as a titbit,  
101 with a thickness of 5 mm and major edge of 10 mm). Cherry had a hemispherical geometry with a  
102 radius of 8 mm, with a spherical hole at the centre (due to destoning) with a radius of 4 mm. The  
103 grape had an ellipsoidal geometry, with major and minor axis of 8 and 5 mm, respectively (**Figure**  
104 **1**). The fruits were inserted into the jar simulating an industrial filling process in the order peach,

105 pear, pineapple, grape and cherry. The jar was then filled with 16.7% (w/w) sucrose solution  
106 measured with an electronic refractometer (Sinotech, Fujian, China). The solid/liquid ratio was  
107 61:39, the same as those of commercial samples. The jar used for the trials had a filling volume of  
108 372 ml, diameter = 86.0 mm; height = 90.5 mm. Glass thickness was measured with a calliper at  
109 different locations on the side and bottom surfaces of the container and resulted in an average value  
110 of 3.5 mm. Prior to experiments, the jar was hermetically closed with a screw metal cap with a  
111 diameter of 85 mm.

112

### 113 *2.3 Data acquisition*

114 The temperatures inside the jar were measured using thermocouples (K-type; Ni/Al-Ni/Cr)  
115 connected to a multimeter acquisition system (Yokogawa Electric Corporation, Tokyo, Japan). A  
116 stainless steel multipoint temperature probe was positioned along the central axis of the jar through  
117 a hole made in the centre of the cap. This multipoint probe (length = 97.5 mm; diameter = 3.5 mm)  
118 included four thermocouples spaced every 13 mm from the tip of the probe in order to record the  
119 syrup temperature at four different heights (17.5, 30.5, 43.5 and 56.5 mm) from the bottom of the  
120 jar. The temperature of fruit pieces was obtained by using five wire thermocouples (diameter = 0.9  
121 mm) inserted at the core of each fruit. The temperature at half the height of the outer wall of the jar  
122 was also measured. Both for multipoint probe and single thermocouples, an acquisition rate of 2 s  
123 was used and time-temperature data were collected in an Excel® ASCII worksheet.

124

## 125 **3. CFD modelling**

### 126 *3.1 Geometry of fruit salad in the glass jar*

127 The process of thermal treatment of fruit salad in a glass jar was simulated by means of a  
128 multidimensional CFD (Computational Fluid Dynamic) model. The observed spatial placement of  
129 the fruit salad inside the container was replicated in a 3D CAD model. In order to reduce the

130 computational effort required by the solution of the CFD model, the spatial domain was assumed to  
131 be symmetric with regard to two perpendicular planes through the vertical axis of the jar, hence  
132 only a quarter of the jar needed to be simulated.

133 The fruit pieces were spatially arranged on a regular grid (8 rows evenly distributed over the full jar  
134 height), and the spacing carefully chosen in order to obtain a solid/liquid content ratio as close as  
135 possible to that measured in the experimental tests. The resulting spatial arrangement of the fruit  
136 pieces in the model of the jar is depicted in **Figure 2**.

137 The model geometry was then imported into the ICEM CFD® software (Canonsburg, Pennsylvania,  
138 USA) and discretized into an unstructured tetrahedral mesh. The maximum element dimension  
139 was chosen taking into consideration the domain (solid, fluid and glass). The values of maximum  
140 element edge dimension for the different fruit pieces inside the jar, together with syrup and glass are  
141 reported in **Table 1**.

142 Following the approach used by Kiziltas et al. (2010) and Dimou et al. (2011), in order to reduce  
143 the complexity of multiphase fluid calculation, the headspace was not considered in the simulation  
144 assuming the jar completely filled with product.

145 In order to accurately calculate the flow field near the wall of the jar, six layers of flat prismatic  
146 wedge element were used for the discretization of the fluid domain. The optimal number of wall  
147 boundary layers needed to obtain an appropriate level of accuracy was identified by means of a  
148 layer-independence analysis, which suggested a value for the dimension of the first element near the  
149 wall equal to 0.04 mm with a height ratio of 1.2 between layers. The final mesh with solid and fluid  
150 elements consists of  $3 \times 10^6$  elements (**Figure 3**).

151

### 152 *3.2 Numerical model*

153 The evaluation of the field of fluid flow and thermal exchange occurring in the considered domain  
154 due to natural convection required numerical solution of the generalized transport equations:

155 a) Continuity Equation

$$156 \quad \frac{\partial \rho}{\partial t} + \nabla \cdot (\rho V) = 0 \quad (1)$$

157 b) Momentum Equation

$$158 \quad \frac{\partial \rho V}{\partial t} + \nabla \cdot (\rho V \cdot V) = \nabla \cdot (-p \delta + \mu(\nabla V + (\nabla V)^t)) + S_M \quad (2)$$

159 c) Energy Equation

$$160 \quad \frac{\partial \rho h_{total}}{\partial t} - \frac{Dp}{Dt} + \nabla \cdot (\rho V h_{total}) = \nabla \cdot (k \Delta T) + S_E \quad (3)$$

161 Where  $t$  is the time,  $V$  is the velocity vector,  $\rho$  is the density,  $p$  is the pressure,  $\mu$  is dynamic  
162 viscosity,  $k$  is thermal conductivity,  $h_{total}$  is the specific total enthalpy.

163 The software Ansys® CFX 14.5 (Canonsburg, Pennsylvania, USA) was chosen for the calculation.

164 Natural convection was modelled using the Boussinesq approximation, which uses a constant  
165 density fluid model, but applies a local body gravitational force throughout the fluid that is a linear  
166 function of thermal expansivity  $\beta$  and of the local temperature difference. The buoyancy source is  
167 added to the momentum equation as follows:

$$168 \quad S_M = -\rho_{REF} \beta (T - T_{REF}) \quad (4)$$

169 Where  $\rho_{ref}$  and  $T_{ref}$  are the density and temperature at the boundary wall condition and  $g$  is the  
170 gravitational force.

171 No internal energy source terms ( $S_E$ ) were taken into account.

172

### 173 3.3 Boundary conditions

174 A uniform time varying temperature condition was applied to all the external surfaces of the jar and  
175 corresponded to that measured in the experimental tests. The value of initial temperature of fruit and  
176 syrup was 22°C, while the variation of the outer wall temperature with time during the heat  
177 treatment is showed in **Figure 4** (black dotted line).

178 Since the maximum Rayleigh number  $Ra$ , as estimated using the maximum temperature difference  
179 and the maximum viscosity, remained lower than  $10^6$  during the whole thermal treatment, laminar  
180 flow was adopted for all the simulations.

181 An adaptive time step option was used in order to maintain the Courant number lower than 1; the  
182 maximum time step of 0.5 s was reached during heating phase. High resolution advection schemes  
183 were adopted for all simulations, in order to achieve second order accuracy. The convergence  
184 criterion was defined as residual root mean square (RMS) value lower than  $10^4$ .

185

### 186 *3.4 Thermal and physical properties*

187 Values of thermal and physical properties such as density ( $\rho$ ), viscosity ( $\mu$ ), specific heat ( $Cp$ ) and  
188 thermal conductivity ( $k$ ) of fruits, syrup and glass were needed for the definition of the model and  
189 the values used are summarized in **Table 1**. The viscosity of the syrup was assumed to be a function  
190 of temperature and a linear interpolation from experimental data was used.

191

### 192 *3.5 Model validation*

193 The developed model was validated by comparing experimental temperature measurements at  
194 specific points inside the glass jar with predicted ones. The accuracy of the model prediction was  
195 assessed by determining root mean square error ( $RMSE$ ) and lethality ( $F_0$ ). The equation for  $RMSE$   
196 determination can be expressed as:

$$197 \quad RMSE = \sqrt{\frac{\sum_{i=1}^n (T_E - T_P)^2}{N}} \quad (5)$$

198 where  $T_P$  is simulated temperature and  $T_E$  is measured temperature, at time  $t$ . The effect of heat  
199 treatment and time with respect to the survival of a microorganism can be quantified by the  
200 following  $F$  value equation (Holdsworth and Simpson, 2007):

$$F = \int_0^t 10^{(T-T_{ref})/z} dt \quad (6)$$

201

202 Lethality was calculated as an equivalent heating time at a constant temperature ( $T_{ref}$ ) of 90°C and a  
203  $z$  value of 10°C as characteristic for pathogenic microorganisms and *Clostridium botulinum* spores  
204 (Padmavati and Anandharamakrishnan, 2013).

205

## 206 **4. Results and discussion**

### 207 *4.1 Validation results*

208 The simulation results were in agreement with the experimental data for both the syrup and the  
209 fruits, as shown in **Table 2**, where validation parameters at each measurement point are reported (4  
210 and 5 points for syrup and fruits, respectively). No significant differences were observed between  
211 experimental and simulated  $F$  values, confirming the accuracy of the developed model. In addition,  
212 in **Figure 4** and **5** heating curves of the experimental treatment and simulation for syrup and fruit  
213 pieces are compared, respectively. The small variations in the results of the model may be due to  
214 the distribution of the fruit pieces, the combined effects of the experimental and model assumptions  
215 such as Boussinesq approximation and the thermal properties of the materials. Furthermore, during  
216 the experiment, the location of the temperature sensor may change the liquid flow pattern and  
217 hence, affects the temperature profile of the sugar solution. In the simulation, small-scale  
218 instabilities were produced by the buoyancy effect. The buoyancy-produced structures might have  
219 directly interacted with the existing local turbulence with the strong coupling where laminar  
220 modelling could not successfully predict this effect.

221

### 222 *4.2 Slowest heating point (SHP) and temperature profile*

223 The identification of the slowest heating point (SHP) inside the container was considered of basic  
224 importance for the effectiveness of thermal processing of our samples. The temperature distribution

225 inside the jar was then measured at different time steps in order to describe the convective  
226 movement of the SHP.

227 When a fluid is subjected to a rapid temperature increase adjacent to a solid wall, part of the fluid in  
228 the wall neighbourhood expands resulting in an increase in the local pressure with significant  
229 effects in heat transfer due to thermal buoyancy effects in a gravitational force field (Aktas and  
230 Farouk, 2003). In a similar way, during thermal processing of solid-liquid mixtures in cans, such as  
231 canned fruit salad, syrup closer to the can walls receives the heat (undergoes heat flux) thus  
232 resulting in volume expansion and density decrease while the syrup far from the walls is still at  
233 lower temperature. This phenomenon leads to development of an upward buoyancy force with a  
234 motion due to density differences. This movement also carries the colder fluid upward by viscous  
235 drag. The fluid flowing upward is deflected by the top surface of the can and starts moving in a  
236 radial direction and, by becoming heavier, starts to move downwards through the stack of fruits.  
237 Consequently, its temperature decreases as it comes in contact with colder pieces of fruits and  
238 syrup, and a new cycle starts from the bottom. These convective movements create a recirculating  
239 flow thus increasing the rate of heat transfer. This observation is similar to the results obtained by  
240 other Authors for natural convection heating mechanism (Ghani et al., 1999a; Padmavati and  
241 Anandharamakrishnan, 2013). The maximum value of liquid velocity was observed close to the  
242 wall of the jar (due to the higher temperature gradient between the jar wall and the thin liquid layer  
243 close to the wall). When solid and impermeable particles were distributed into the fluid, the velocity  
244 profile changed due to the heat exchange and surface deflections: the flow was very slow through  
245 the stack of solid particles in the horizontal direction while on the contrary it showed an increase  
246 between solids in the vertical direction.

247 In the case of pure convection heating of liquids, the slowest heating point (SHP) is located at about  
248 10-15% of the can height (Padmavati and Anandharamakrishnan, 2013), but in the case of solid-  
249 liquid food mixtures heated by a combination of conduction and convection, SHP location is more

250 complex to determine. Under our experimental conditions, the SHP of the canned fruit salad was  
251 not at the geometric centre of the can nor at a can height of 10-15% but at an intermediate position  
252 between these (19-20% of the can height). The position of SHP is well shown by the *F value* of the  
253 various fruits: pear pieces presented the lowest *F value* because this kind of fruit was positioned  
254 closer to the SHP.

255 The natural convection effects also influenced the heating of the fruit pieces. As shown in **Table 2**,  
256 the fruits positioned close to the top of the jar showed a simulated *F value* higher than those placed  
257 close to the bottom: grape = 8.80 min, peach = 4.16 min.

258 When there is a marked effect of natural convection heating, thermal stratification takes place  
259 (observation based on the fluid movement due to buoyancy effects explained above). **Figure 6**  
260 shows temperature stratification for the syrup during heating phase, at 4 different time steps (5, 10,  
261 20 and 30 min), while **Figure 7** reports the temperature stratification along the fruit pieces at the  
262 same time steps (both figures come from the graphical representation of the mathematical model).

263

## 264 **5. Conclusions**

265 In this study, a 3D CFD model was developed in order to investigate the temperature profiles, to  
266 identify the slowest heating point (SHP) and to describe the flow field during the heating processing  
267 of canned fruit salad composed of five kinds of fruit canned in a glass jar and filled with sugar  
268 syrup.

269 Experimental *F values* were different among the various fruits and in particular they were a  
270 function of position, dimension and thermal properties; moreover, experimental *F values* were also  
271 greatly influenced by the natural convection motion of the syrup.

272 Concerning the proposed model, an appreciable agreement between simulated and experimental  
273 measurements of temperature both for syrup and fruit pieces was obtained: the model can be



274 considered successfully validated and applicable for the simulation and prediction of thermal  
275 processes of canned fruit salad.  
276 An increase in the reliability of the model by minimizing the differences with experimental data and  
277 by studying the influence of fruit position inside the jar during the thermal process can be achieved.

278 **References**

- 279 Akhijahani, H. S., Khodaei, J. (2013). Investigation of specific heat and thermal conductivity of  
280 rasa grape (*Vitis vinifera* L.) as a function of moisture content. *World Applied Sciences Journal*, 22,  
281 939-947.
- 282 Aktas, M.K., Farouk, B. (2003). Numerical simulation of developing natural convection in an  
283 enclosure due to rapid heating. *International Journal of Heat and Mass Transfer*, 46, 2253-2261.
- 284 Anandharamakrishnan, C. (2011). Applications of computational fluid dynamics in food processing  
285 operations. In A. D. Murphy (Ed-), *Computational fluid dynamics: theory, analysis and*  
286 *applications-Chapter 9* (pp. 297-316). New York: Nova Publishers.
- 287 ASHRAE, (2006). Thermal properties of foods. *Handbook refrigeration-Chapter 9*.
- 288 Chen, C.R., & Ramaswamy, H.S. (2007). Visual basic computer simulation package for thermal  
289 process calculations. *Chemical Engineering and Processing*, 46, 603-613.
- 290 Chhanwal, N., Tank, A., Raghavarao, K.S.M.S., & Anandharamakrishnan, C. (2012).  
291 Computational fluid dynamics applications in bread baking process. *Food and Bioprocess*  
292 *Technology*, 5, 1157-1172.
- 293 Dimou, A., Yanniotis, S. (2011). 3D numerical simulation of asparagus sterilization in a still can  
294 using computational fluid dynamics. *Journal of Food Engineering*, 104, 394-403.
- 295 Ghani, A. G., & Farid, M. M. (2006). Using the computational fluid dynamics to analyse the  
296 thermal sterilization of solid-liquid food mixture in cans. *Innovative Food Science and Emerging*  
297 *Technologies*, 7, 55-61.
- 298 Ghani, A. G., Farid, M. M., & Chen, X. D. (2002). Numerical simulation of transient temperature  
299 and velocity profiles in a horizontal can during sterilization using computational fluid dynamics.  
300 *Journal of Food Engineering*, 51, 77-83.

301 Ghani, A. G., Farid, M. M., Chen, X. D., & Richards, P. (1999a). Numerical simulation of natural  
302 convection heating of canned food by computational fluid dynamics. *Journal of Food Engineering*,  
303 41, 55-64.

304 Ghani, A. G., Farid, M. M., Chen, X. D., & Richards, P. (1999b). An investigation of deactivation  
305 of bacteria in canned liquid food during sterilization using computational fluid dynamics (CFD).  
306 *Journal of Food Engineering*, 42, 207-214.

307 Holdsworth, D., Simpson, R. (2007). *Thermal processing of packaged foods, food engineering*  
308 *series*. New York: Springer.

309 Incropera, F. P, DeWitt D. P., Bergman T. L., Lavine, A. S. (2006). *Fundamental of heat and mass*  
310 *transfer*. John Wiley & Sons.

311 Kiziktas, S., Erdogdu, F., & Palazoglu, T.K. (2010). Simulation of heat transfer for solid-liquid  
312 food mixtures in cans and model validation under pasteurization conditions. *Journal of Food*  
313 *Engineering*, 97, 449-456.

314 Kumar, A., Bhattacharya, M., & Blaylock, J. (1990). Numerical simulation of natural convection  
315 heating of canned thick viscous liquid food products. *Journal of Food Science*, 55, 1403-1411.

316 Kuriakose, R., & Anandharamakrishnan, C. (2010). Computational fluid dynamics (CFD)  
317 applications in spray drying of food products. *Trends in Food Science and Technology*, 21, 383-  
318 398.

319 Norton, T., Sun, D.W. (2006). Computational fluid dynamics (CFD) – an effective and efficient  
320 design and analysis tool for the food industry: A review. *Trend in Food Science & Technology*, 17,  
321 600-620.

322 Padmavati, R., Anandharamakrishnan, C. (2013). Computational Fluid Dynamics Modeling of the  
323 Thermal Processing of Canned Pineapple Slices and Titbits. *Food Bioprocess Techology*, 6, 882-  
324 895.

325 Rabiey, L., Flick, D., & Duquenoy, A. (2007). 3D simulations of heat transfer and liquid flow  
326 during sterilization of large particles in a cylindrical vertical can. *Journal of Food Engineering*, 82,  
327 409-417.

328 Rahman, M.S. (2008). *Food properties Handbook*. Boca Raton: CRC.

329 Sun, D.W. (2007). *Computational fluid dynamics in food processing*. Boca Raton: CRC.

330 Varma, M. N., & Kannan, A. (2005). Enhanced food sterilization through inclination of the  
331 container walls and geometry modifications. *International Journal of Heat and Transfer*, 48, 3753-  
332 3762.

333 Weng, Z.J. (2005). Thermal processing of canned foods. In: Sun, Da-Wen (Ed.), *Thermal Food*  
334 *Processing-New Technologies and Quality Issues – Chapter 11*. Boca Raton: CRC-Taylor and  
335 Francis.

336 Whitelock, D.P., Brusewitz, G.H., Ghajar, A.J. (1999). Thermal/physical properties affect predicted  
337 weight loss of fresh peaches. *American Society of Agricultural Engineers*, 42, 1047-1053.

338 Xia, B., & Sun, D.W. (2002). Review: applications of computational fluid dynamics (CFD) in the  
339 food industry. *Computers and Electronics in Agriculture*, 34, 5-24.

Figure 1  
[Click here to download high resolution image](#)

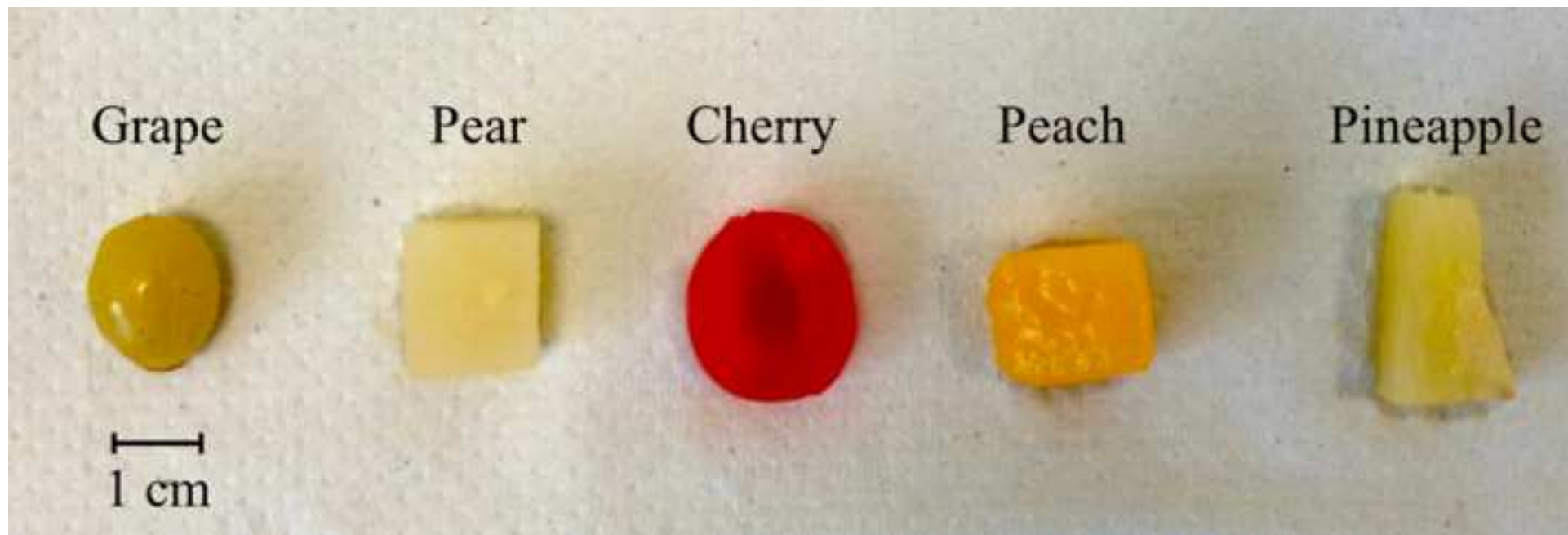


Figure 2  
[Click here to download high resolution image](#)

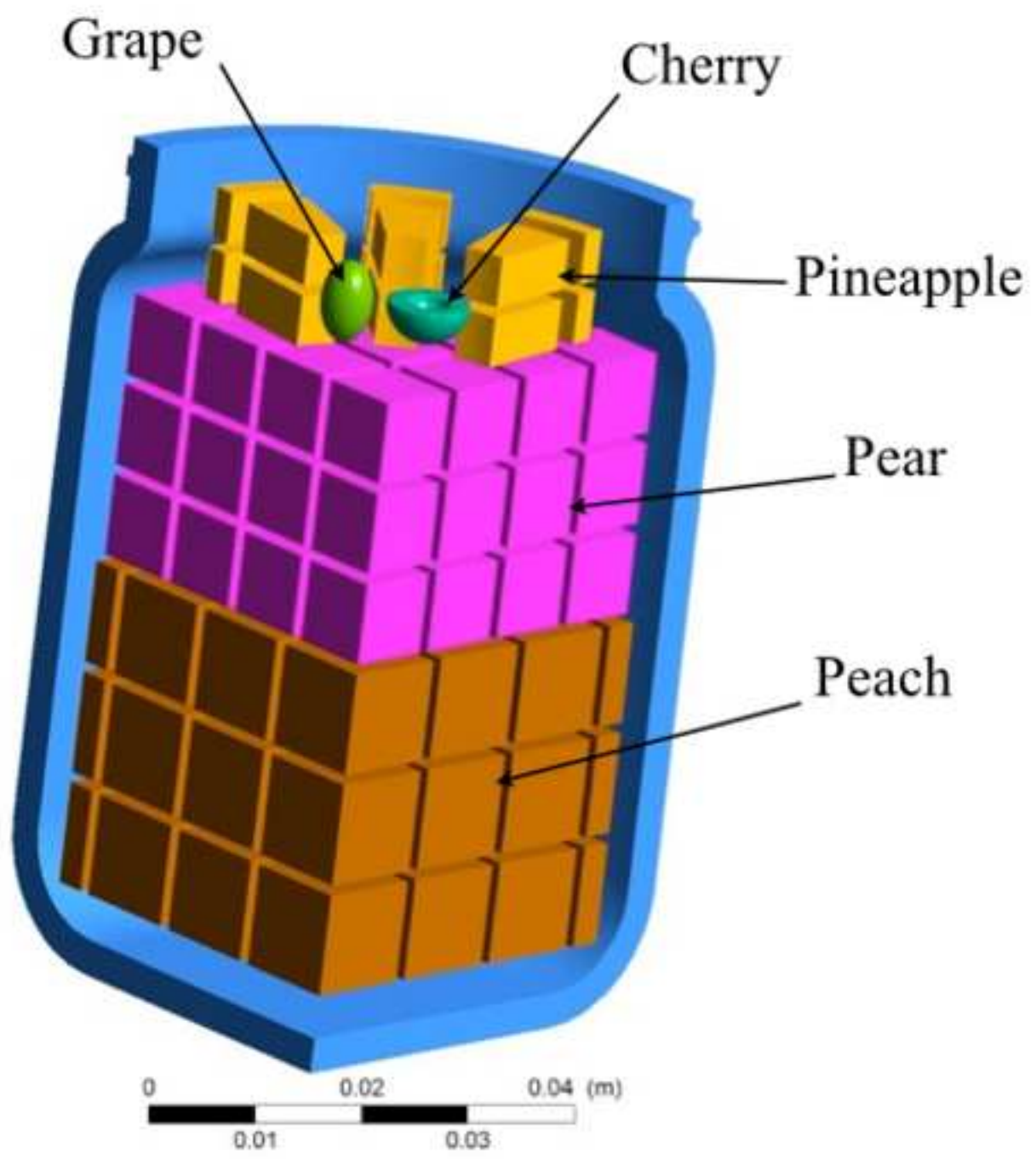


Figure 3  
[Click here to download high resolution image](#)

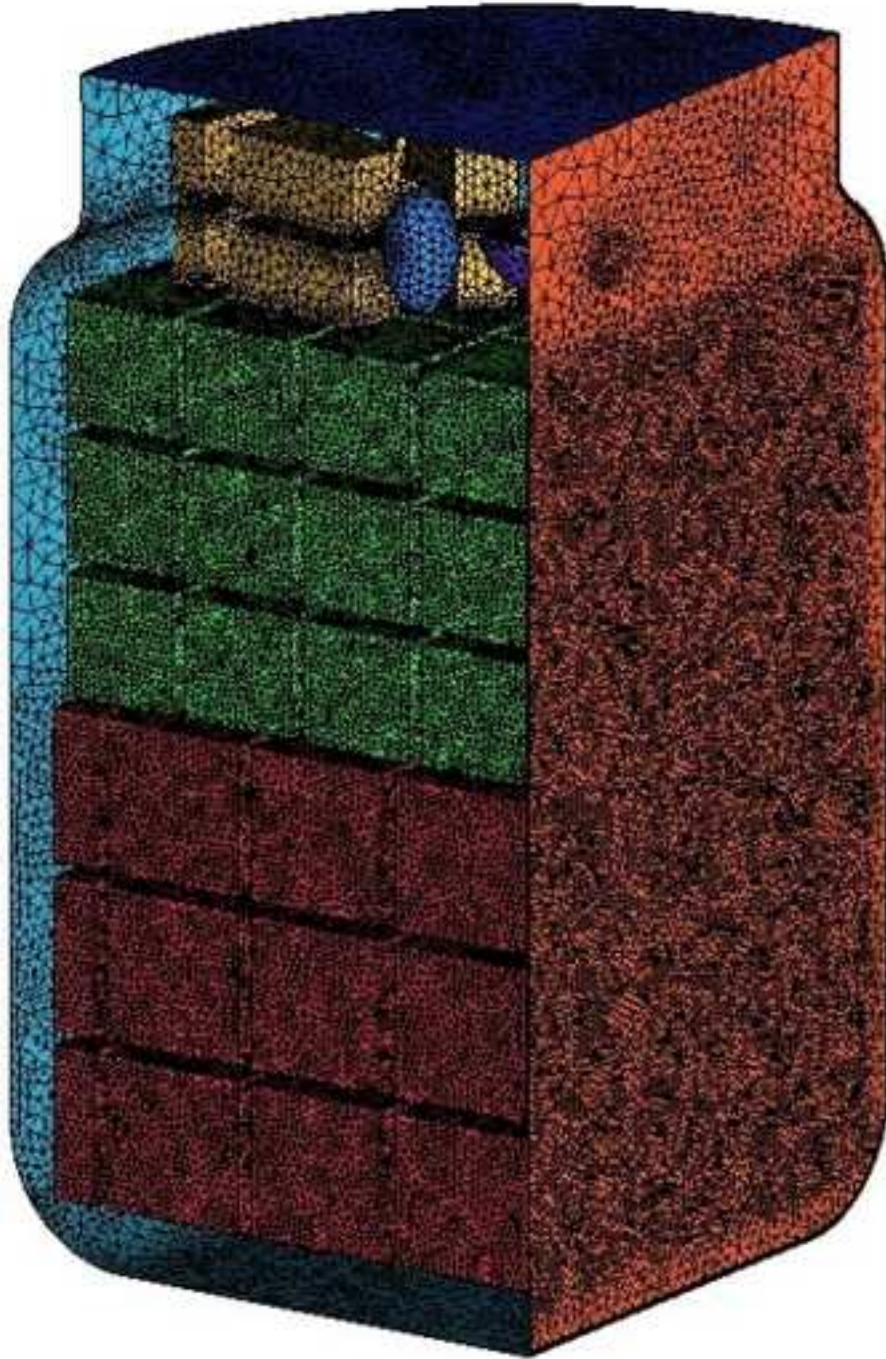


Figure 4  
[Click here to download high resolution image](#)

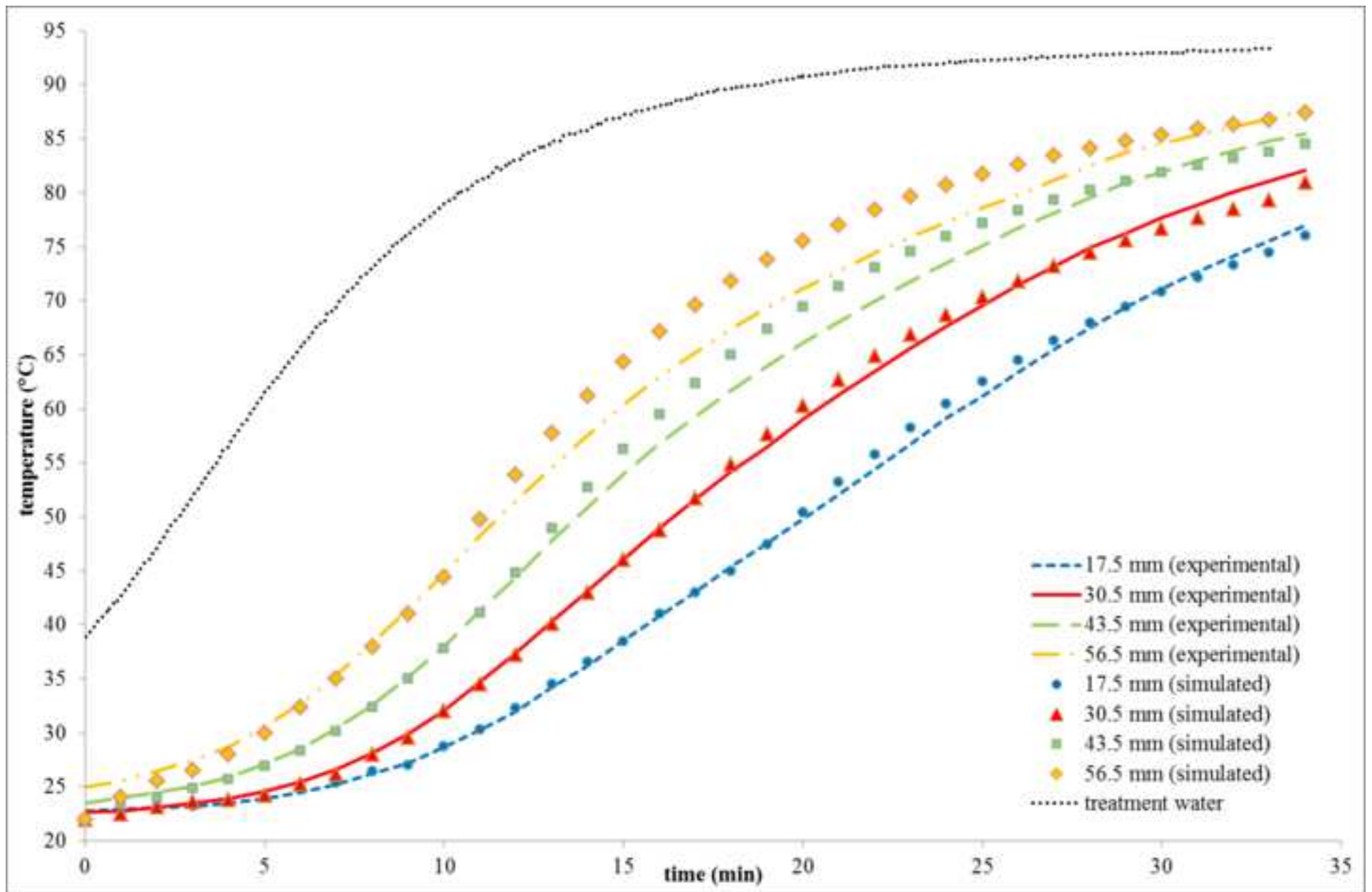




Figure 5  
[Click here to download high resolution image](#)

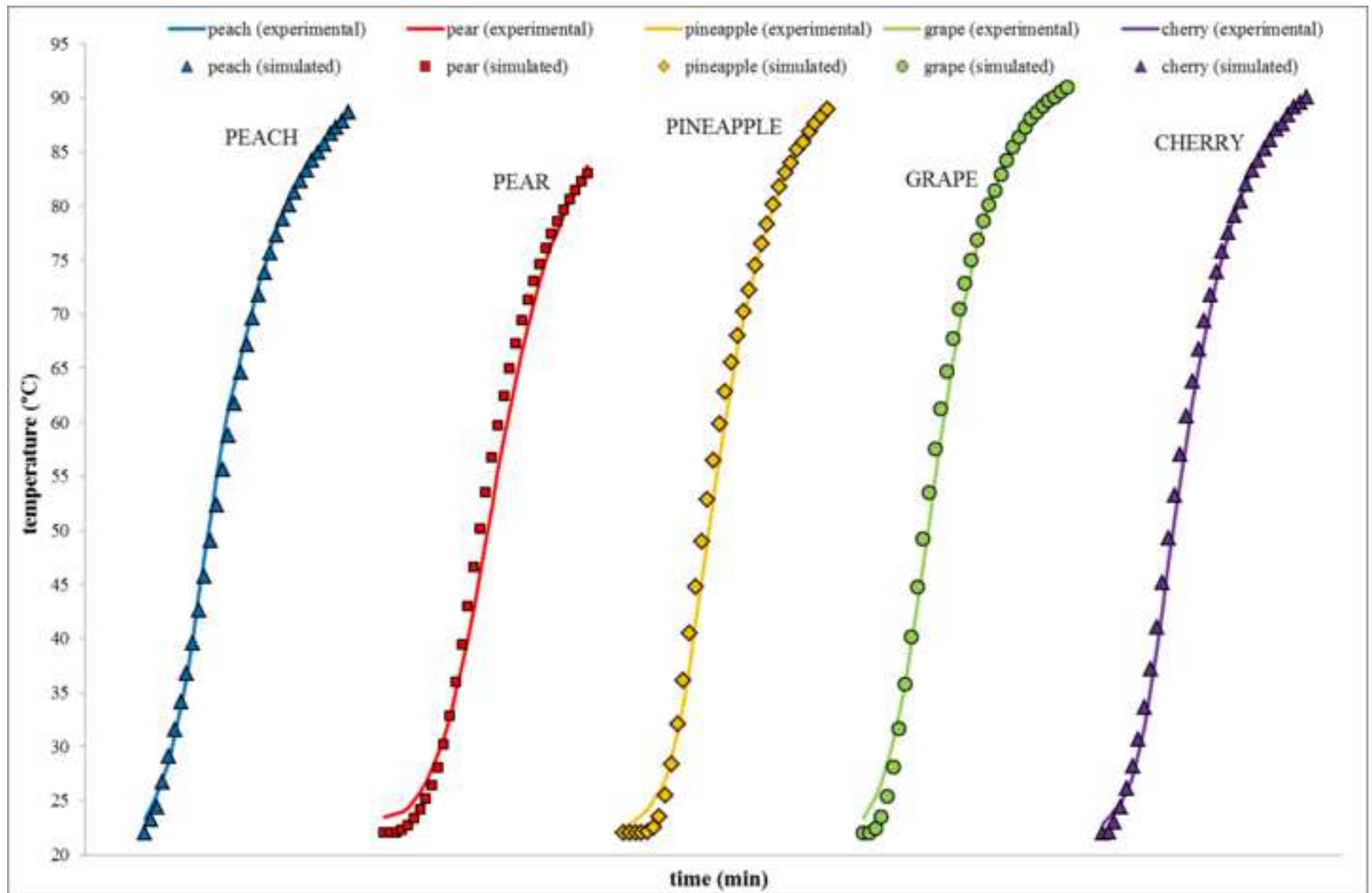


Figure 6  
[Click here to download high resolution image](#)

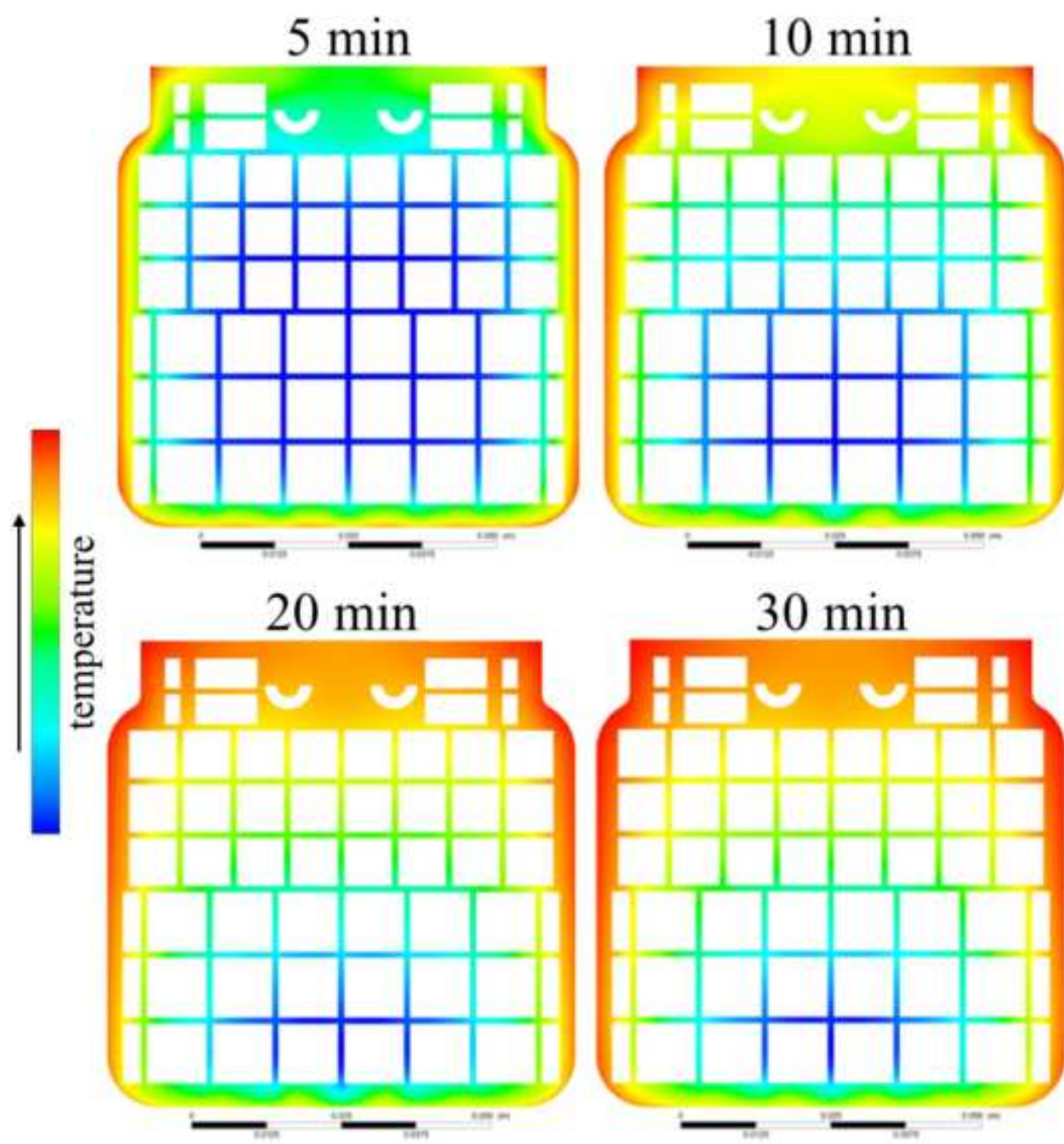
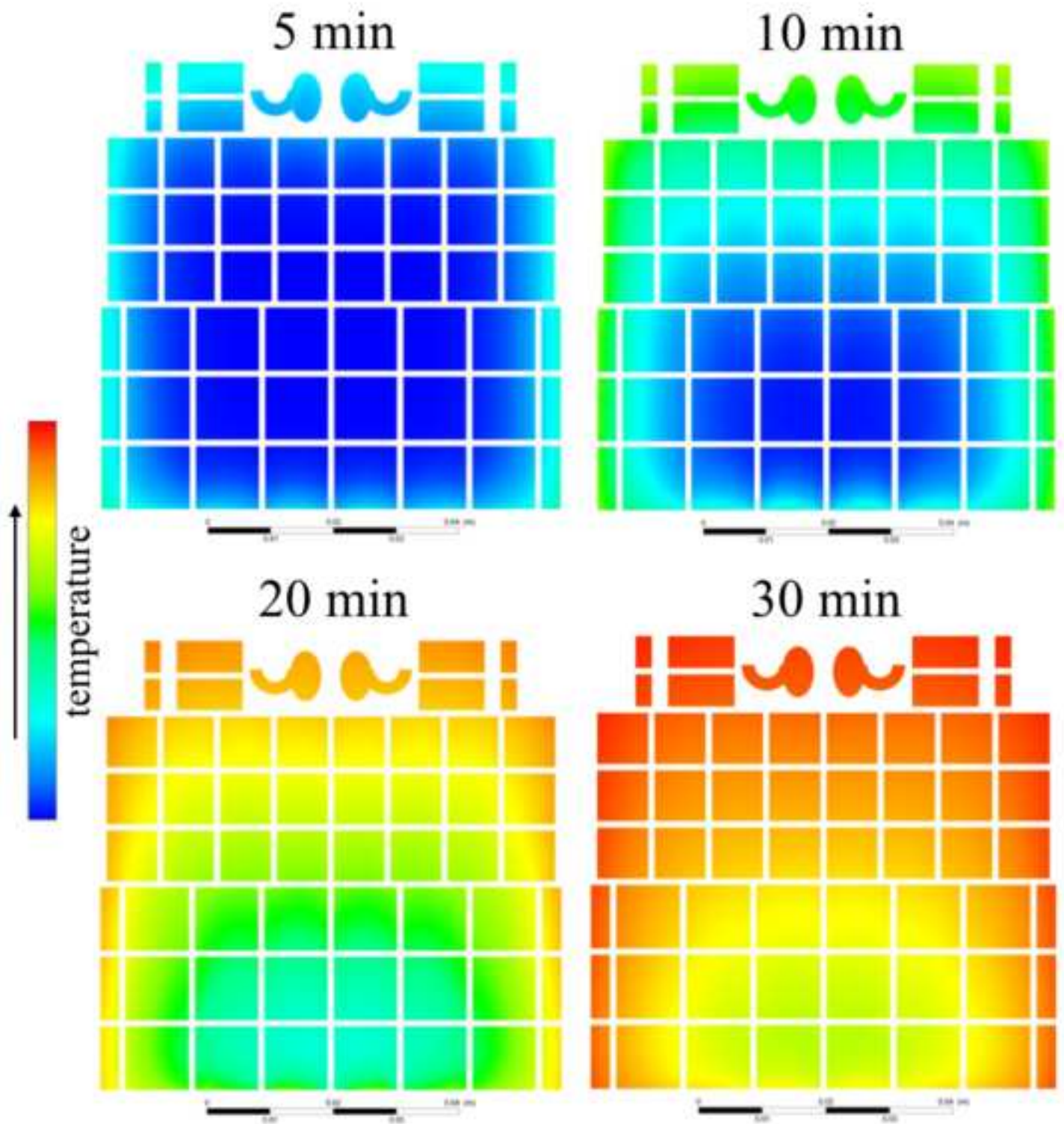


Figure 7  
[Click here to download high resolution image](#)



### **Captions for Figures and Tables**

**Fig. 1** - Visual comparison of the different kind of fruits used in the experiments

**Fig. 2** - 3D model of the distribution of the fruits inside the jar

**Fig. 3** - 3D model of the fruits inside the jar with the mesh element

**Fig. 4** - Comparison of temperature profile in syrup between experimental test and mathematical model

**Fig. 5** - Comparison of the temperature profile in fruit pieces between experimental test and mathematical model

**Fig. 6** - Temperature stratification of the syrup at 4 different time steps (from mathematical model)

**Fig. 7** - Temperature stratification of the fruit pieces at 4 difference time steps (from mathematical model)

**Table 1** - Thermal properties, rheological characteristic and maximum element edge dimension for all the different kinds of fruit inside the jar, together with syrup and glass

**Table 2** - Validation results

**Table 1**

Food	$\rho$ (kg/m <sup>3</sup> )	$\mu$ (Pa s)	$C_p$ (J/kg K)	$k$ (W/m K)	<i>Max edge length<sup>g</sup> (mm)</i>
Syrup (16,7% sugar)	1074 <sup>g</sup>	0,0258-0,00023*T <sup>g</sup>	-	-	0.50
Peach	930 <sup>a</sup>	-	3700 <sup>a</sup>	0.581 <sup>b</sup>	1.70
Pear	1000 <sup>b</sup>	-	3800 <sup>c</sup>	0.595 <sup>b</sup>	1.50
Pineapple	1010 <sup>d</sup>	-	3490 <sup>d</sup>	0.549 <sup>d</sup>	0.80
Grape	1320 <sup>c</sup>	-	3325 <sup>e</sup>	0.273 <sup>e</sup>	0.45
Cherry	1049 <sup>b</sup>	-	3730 <sup>c</sup>	0.511 <sup>c</sup>	0.26
Glass	2500 <sup>f</sup>	-	750 <sup>f</sup>	1.400 <sup>f</sup>	2.00

<sup>a</sup> from Whitelock et al. (1999);

<sup>b</sup> from Rahman (2008);

<sup>c</sup> from 2006 ASHRAE Handbook-refrigeration;

<sup>d</sup> from Padmavati and Anandharamakrishnan (2013);

<sup>e</sup> from Akhijahani and Khodaei (2013);

<sup>f</sup> from Incropera et al. (2006);

<sup>g</sup> experimental value.

Table 2

<i>Point of measurement</i>		<i>RMSE</i>	<i>Lethality (<math>F_{90,10}</math>)</i>		
			<i>Experimental</i>	<i>Simulated</i>	$\Delta F_{90,10}$
Syrup	17,5 mm	0.68	0.17	0.14	0.02
	30,5 mm	0.79	0.66	0.52	0.14
	43,5 mm	1.77	1.68	1.62	0.05
	56.5 mm	2.65	2.99	3.73	0.73
	<b>Average</b>	<b>1.47</b>			<b>0.13</b>
Peach		1.14	4.24	4.16	0.07
Pear		2.31	0.95	0.96	0.02
Pineapple		1.78	4.04	4.13	0.09
Grape		1.61	8.87	8.80	0.06
Cherry		1.31	6.24	6.27	0.03
<b>Average</b>		<b>1.63</b>			<b>0.06</b>